PHYSICAL REVIEW B

CONDENSED MATTER

THIRD SERIES, VOLUME 26, NUMBER 10 15 NOVEMBER 1982

Finite-wavelength effects in composite media

W. G. Egan
Research and Development Center, Grumman Aerospace Corporation, Bethpage, New York 11714

D. E. Aspnes
Bell Laboratories, Murray Hill, New Jersey 07974

(Received 9 July 1982)

We report wavelength- (λ-) and size-dependent measurements of the dielectric functions (ϵ) of macroscopically uniform samples pressed from Al_2O_3 powders of different particle sizes. The data agree with effective medium (mean-field) theories for particle diameters less than about 0.25λ. For particle diameters larger than about 0.5λ, measured values of ϵ exceed allowable quasistatic limits for known volume fractions, and finite-wavelength effects must be considered. We show that finite-wavelength theories are more sensitive to microstructural parameters than quasistatic theories, which suggests that finite-wavelength models should be useful for microstructural or materials characterization and could also have predictive value. Finally, we show that the recent perturbation model of Bosi, Girouard, and Truong, that includes dynamic terms as additions to a quasistatic theory, predicts rates of increase of ϵ with particle size that greatly exceed those of experiment or other model calculations. Thus dynamic terms cannot in general be incorporated as additions to quasistatic theories but must be included in the initial formulation of the effective-medium problem.

I. INTRODUCTION

The description of the dielectric properties of heterogeneous or composite materials is a historic problem that has attracted considerable recent attention.[1] In such materials, an externally applied field causes a screening charge to accumulate at the boundaries between the separate phases. The screening charge generates differences in the local fields and polarizations from their macroscopic average, or observable, counterparts. Because the importance of screening depends on a number of factors such as the difference in polarizability of the separate phases, their relative volume fractions, the sizes and shapes of the individual regions, and the presence or absence of macroscopic isotropy, the calculation of the dielectric function ϵ of a heterogeneous material can be performed accurately only if the microstructure is known in detail.

This knowledge is typically unavailable analytically for real systems where the microstructure is essentially random. Nevertheless, considerable progress has been made in the limit where the characteristic dimensions of the microstructure are small compared to λ, the wavelength of the radiation. In this limit, the time dependence can be ignored and the local fields and polarizations can be calculated in principle from the "electrostatic" continuity conditions on local displacement and electric fields $\vec{d}(\vec{r})$ and $\vec{e}(\vec{r})$, respectively. Numerous effective-medium or mean-field expressions of varying degrees of detail and complexity have been developed in this approximation,[2–10] and rigorous (and fairly restrictive) limit theorems have been derived for the allowed range of ϵ for the special case of two-component composites.[11–14] General expressions[15] and discussions of the relationships among various quasistatic theories[16–19] can be found in the literature. Within the microstructural size limitation, these models give a satisfactory account of the experimental results for a wide range of systems,[17,20–29] provided that suitable averages are taken over size and shape distributions; also the decrease of the mean free path due to surface scatter-

ing must be taken into account in systems containing small metal particles.

In contrast to the quasistatic case, the analytical and experimental situations where the microstructural dimensions are comparable to λ are much less clear. This more difficult problem has received theoretical attention only very recently,[30–36] and quantitative data on fully characterized samples are virtually nonexistent. While it is known that quasistatic theories can give a reasonable characterization of the spectral response of composites whose microstructural dimensions are too large for these theories to be rigorously applied,[37–39] it is not clear that the parameters, such as volume fractions and particle shapes, that reproduce these spectral responses are really representative of the samples. Indeed, there is reason to suspect that the naive application of quasistatic models can lead to significant systematic errors. It was recently shown[35] that refractive indices measured[38] for pressed-powder composites of known packing fraction exceeded the maximum values allowed by quasistatic-limit theorems for samples for which microstructural dimensions were of the order of λ. Exact solutions for laminar microstructures[35] indicated that a waveguiding effect that favored propagation in the more dense phase was the responsible mechanism.

In view of the variety of conflicting theories of limited applicability, there is a clear and pressing need to obtain quantitative data on samples well characterized with respect to all relevant parameters: the dielectric functions and volume fractions of the constituent phases and the sizes and shapes of the separate composite regions. It has been our objective to provide such data for composite systems consisting of Al_2O_3 and voids. This choice was dictated by practical reasons. First, dimensionally well-characterized Al_2O_3 particles of various sizes are readily available as abrasives. Second, the intrinsic dielectric properties of the oxide are essentially determined by intra-atomic electronic transitions between the nonbonding oxygen $2p$ levels and the oxygen $3s$ levels of the lower conduction band and consequently are little affected by particle size and shape or by crystalline quality. Third, the material is transparent in the visible to the near uv spectral range, which simplifies calculations by allowing one to work with real variables; more importantly, the transparency property provides a genuine test of finite-wavelength theories because the light is

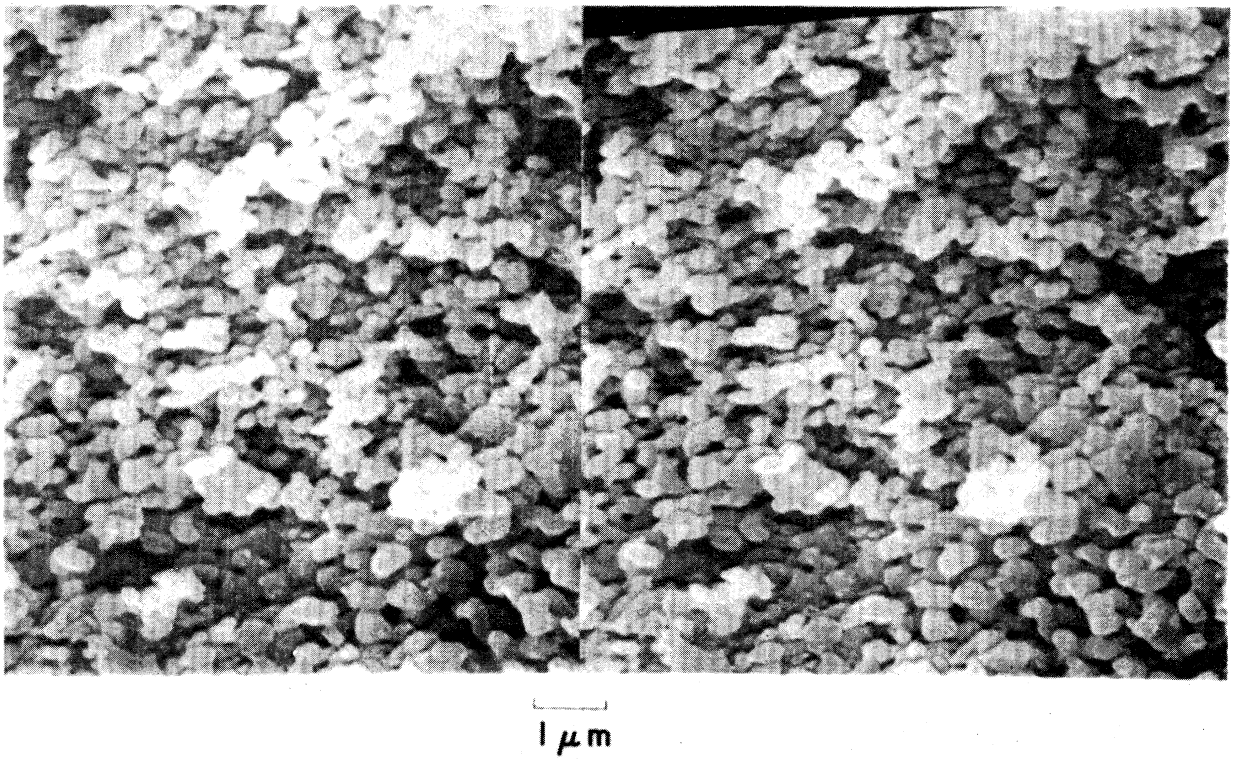

FIG. 1. Stereographic SEM micrographs of the front surface of a pressed-powder composite prepared from 0.3-μm alumina abrasive. The surface can be seen in three dimensions by using a stereo viewer.

able to sample appreciable distances of the composite. In contrast, surface effects dominate in strongly absorbing materials where the penetration depths are small. Fourth, the low dispersion of Al_2O_3 allows us to exploit a variable not previously used. We can parametrically change the particle dimension to wavelength ratio of a given sample by changing λ with the certainty that the microstructure is invariant and the optical properties nearly so.

II. EXPERIMENT

Composite samples were prepared by compressing corundum abrasive powders of nominal particle sizes of 0.05-, 0.3-, 1.0-, and 3.0-μm diameters between 13-mm diameter hardened steel dies as described previously.[38] Particles 3.0 μm in size were obtained as Microabrasives Microgrit WCA. The other sizes were obtained as Linde *A*, *B*, and *C*. The 0.05-μm particles were 15% α phase and 85% γ phase, and the 0.3-μm particles were 90% α phase and 10% γ phase as verified by x-ray-diffraction measurements. The 1.0- and 3.0-μm particles were entirely α phase. Because of their great hardness, no shape or phase change of the particles was expected from compression during sample preparation.

Packing or volume fractions were determined from the measured mass and volume of each pellet. The uniformities of particle size and shape and of the microstructure of the compressed pellets were characterized by a combination of scanning electron microscope (SEM) and sedimentation measurements. An SEM micrograph of a typical sample prepared from 0.3-μm particles is shown in stereogram form in Fig. 1. The individual particles are in the form of platelets, but the distribution is completely random and macroscopically uniform over the field of view. All samples exhibited this type of macroscopic homogeneity, not only at the surface but throughout the bulk as verified by SEM micrographs of fractured samples.

With respect to the other materials, the 0.05-μm particles were found to be of the specified size, but they tended to agglomerate into platelet structures. The 1.0-μm particles were ellipsoidal and also formed platelet agglomerates. These samples also appeared to contain a significant amount of fines of less than 1.0-μm diameter. The nominal 3.0-μm particles were platelets with less than 1% of fines less than 1.0 μm or larger than 10 μm in size.

Values of ϵ were calculated from refractive indices measured at wave lengths $\lambda=6328$, 6000, 5000, 4000, 2800, and 2000 Å using the Brewster-angle method[40] on the quasispecular large-area surfaces of the compressed pellets. The 6328-Å observations were made with a HeNe laser. The remaining data were obtained using tungsten-halogen (6000,5000,4000 Å) and high-pressure HgXe arc (2800,2000 Å) sources together with a modified Perkin-Elmer model-13*U* spectrograph and suitable filters. The wavelength resolution was 0.05 μm. The illuminated areas were 13-mm diameter, and 13- and 0.8-mm diameter for the laser with and without beam expander, respectively.

The measured laser beam divergence was 1.6 mrad, while that for the other illumination systems was 17 mrad. For the large diameter incident beams, the aperture stop of the sensor system was adjusted to accept radiation scattered from a 2-mm-diameter sample area. The aperture stop was removed when the direct laser beam was used. The rationale for the optical geometry will be discussed in a following section.

III. THEORY

The general concept of a dielectric function has validity in describing the response of a medium to an electromagnetic perturbation only in an average sense. The conditions under which this can be done are discussed in detail by Stroud and Pan[32] and by Lamb, Wood, and Ashcroft.[34] Difficulties do not arise in the quasistatic (infinite-wavelength) limit where the natural length scale $1/|\vec{k}|$ of the electromagnetic radiation is much larger than the other two length scales relating to the microstructure and to the averaging process. Thus difficulties arise when $1/|\vec{k}|$ and the microstructural dimensions become comparable, and scattering effects cannot be ignored. A natural method of defining a dielectric function in this context is to consider the wave vector associated with mean propagation or forward scattering, whereby if ϵ is properly chosen, the forward scattering should vanish. Under this condition[32]

$$\int_v \vec{d}(\vec{r},\omega)e^{-ikz}d\vec{r}=\epsilon\int_v \vec{e}(\vec{r},\omega)e^{-ikz}d\vec{r}\,, \quad (1)$$

where $\vec{d}(\vec{r},\omega)$ and $\vec{e}(\vec{r},\omega)$ are the microscopic displacement and electric fields, respectively, and $\epsilon=c^2k^2/\omega^2$ is the scalar dielectric function of the composite medium. In Eq. (1) propagation is assumed to be in the z direction.

For two-phase composites, the common quasistatic models and limit theorems can be summarized concisely as[15]

$$\epsilon=\frac{q\epsilon_a\epsilon_b+(1-q)\epsilon_h(f_a\epsilon_a+f_b\epsilon_b)}{(1-q)\epsilon_h+q(f_a\epsilon_b+f_b\epsilon_a)}\ , \tag{2}$$

where ϵ_a,ϵ_b and f_a,f_b are the dielectric functions and volume or packing fractions of the separate phases a,b, q $(0\le q\le 1)$ is a screening parameter, and ϵ_h is a "host" dielectric function that will be assigned to one, or the other, or some combination of, the dielectric functions of the separate phases. The volume fractions satisfy the conditions $0\le f_a,f_b\le 1$, $f_a+f_b=1$. The absolute Wiener limits[11] to the allowed range of ϵ for arbitrary composition and microstructure are obtained for $q=0$ or 1 and $0\le f_a\le 1$. The Hashin-Shtrikman limits[12] for known macroscopic composition are defined by f_a and $0\le q\le 1$. The Bergman-Milton limits[13,14] for known composition and two- $(q=\frac{1}{2})$ or three-dimensional $(q=\frac{1}{3})$ macroscopic isotropy are obtained by fixing f_a, q, and imposing the Wiener limits on ϵ_h. The Maxwell-Garnett expressions[3] follow by taking $\epsilon_h=\epsilon_a$ or ϵ_b, while the Bruggeman effective-medium approximation (EMA)[4] is obtained with the self-consistent choice $\epsilon_h=\epsilon$. We shall use the Bruggeman expression to compare data to quasistatic theory.

A number of approaches have been developed to deal with finite-wavelength effects. We shall work with the exact expressions, as well as with their quadratic expansions in d/λ. The simplest of these is the two-phase (superlattice) laminar model,[35] which is the finite-wavelength solution of Eq. (1) for the microstructures that lead to the absolute Wiener limits in the quasistatic case [Eq. (2)]. This theory is not expected to apply to our samples, which have an essentially random microstructure, but it should provide an estimate of the limiting theoretical behavior in the finite-wavelength case. The quadratic expansion of the equations describing this model microstructure can be written

$$\epsilon(d/\lambda)\cong\epsilon+\frac{\pi^2(\epsilon_a-\epsilon_b)^2\zeta_a\zeta_b d_a^2 d_b^2}{3\lambda^2(d_a\zeta_b+d_b\zeta_a)^2}\ , \tag{3}$$

where d_a and d_b are the thicknesses of the laminations of phases a and b. For the TE mode $\zeta_a=\zeta_b=1$ and $\epsilon=f_a\epsilon_a+f_b\epsilon_b$, while for the TM mode $\zeta_a=\epsilon_a,\zeta_b=\epsilon_b$, and $1/\epsilon=f_a/\epsilon_a+f_b/\epsilon_b$. Note that the quasistatic limits converge to the two Hashin-Shtrikman limits, which define the allowed range of ϵ when f_a is known.

A similar quadratic expansion can be developed for spherical inclusions, as given by Stroud and Pan.[32] Here, Eq. (1) is solved in a dynamic effective-medium approximation (DEMA) using the standard Mie coefficients[41] for scattering from spherical particles. From Eq. (3.2) of Ref. 32 we find

$$\epsilon(d/\lambda)\cong\epsilon+\frac{\sum_i \frac{\pi^2 d_i^2}{30\lambda^2}f_i(\epsilon_i-\epsilon)}{\frac{3f_a\epsilon_a}{(\epsilon_a+2\epsilon)^2}+\frac{3f_b\epsilon_b}{(\epsilon_b+2\epsilon)^2}}\ , \tag{4}$$

where f_i and ϵ_i are the volume fractions and dielectric functions of all particles of diameter d_i. The quasistatic limit ϵ in this case is just that of the self-consistent Bruggeman EMA theory. In Eq. (4), the correction term arises entirely from magnetic dipole effects, and it can vary over a considerable range depending on the relative diameters of the spherical regions. More general expressions can be derived from the multipole-modified Maxwell-Garnett expressions of Lamb *et al.*[34] However, these are based on the same principles so we shall use Eq. (4) as a representative special case.

The laminar and spherical-inclusion expressions are examples based on DEMA theories. Recently, Bosi *et al.*[36] proposed another approach, that of treating finite-wavelength effects as perturbations to the quasistatic formalism. The expressions given in Ref. 36 are not directly applicable without some modification: They were developed for two-dimensional systems and include self-consistent dipolar and quadrupolar polarization terms $\vec{E}_d$ and $\vec{E}_q$ that vanish in random three-dimensional systems. However, the necessary modifications are straightforward. Equations (34), (38), and (39) of Ref. 36 are simply replaced with

$$\vec{E}_{\rm loc}=\vec{E}_e\ , \tag{5a}$$

$$\vec{P}=\vec{P}_{||}=\vec{P}_{\perp}=\frac{3}{4\pi}f_a\Delta_1\vec{E}\ , \tag{5b}$$

where f_a is the volume fraction occupied by the spherical particles of dielectric function ϵ_a. The quantity Δ_1 is defined for dipolar and quadrupolar interactions in Appendixes *A* and *B* of Ref. 36. From Eqs. (5) above and Eqs. (33), (40), and (41) of Ref. 36, it follows that

$$\epsilon(d/\lambda)=\epsilon+\frac{\pi^2}{18}\left[\frac{d}{\lambda}\right]^2 f_a(\epsilon+2)^2\times\left[\frac{79\epsilon_a^2-112\epsilon_a+36}{5(\epsilon_a+2)^2}+\frac{\epsilon_a-1}{2\epsilon_a+3}\right], \tag{6}$$

where the host medium is assumed to be empty

TABLE I. Measured values of ϵ for various compressed pellets discussed in text, with corresponding physical parameters: particle size d, (μm) packing fraction f_a, ϵ (EMA at 5000 Å), ϵ_{EMA}; index of refraction for Al_2O_3 (from Ref. 40), n_0; radiation wavelength λ (Å).

		$d=0.05$ $f_a=0.47$ $\epsilon_{\mathrm{EMA}}=1.88$	$d=0.3$ $f_a=0.57$ $\epsilon_{\mathrm{EMA}}=2.13$	$d=1.0$ $f_a=0.46$ $\epsilon_{\mathrm{EMA}}=1.86$	$d=3.0$ $f_a=0.62$ $\epsilon_{\mathrm{EMA}}=2.26$
$\lambda=6328$	$n_0^2=3.335$	1.918	2.637	1.357	2.723
$\lambda=6000$	$n_0^2=3.341$		2.931		
$\lambda=5000$	$n_0^2=3.366$	2.005	3.467	2.190	2.958
$\lambda=4000$	$n_0^2=3.411$	1.946	3.675	2.531	2.979
$\lambda=2800$	$n_0^2=3.554$	1.907	3.591	2.762	3.233
$\lambda=2000$	$n_0^2=3.892$	1.949	3.561	2.654	3.014

space ($\epsilon_b=1$), d is the diameter of the equivalent spherical inclusions, and the quasistatic limit ϵ is calculated in the Maxwell-Garnett approximation with b (void) being the host phase. In Eq. (6), the first and second terms in second large parentheses represent the magnetic dipole and electric quadrupole contributions, respectively.

Another approach was developed by Ruppin[31] to deal with apparent absorption, that is, the loss of flux in the forward direction due to scattering. The theory is intended for transmission measurements and thus is not applicable to our measurements. Likewise, the retarded-potential generalization of the Maxwell-Garnett expression by Granqvist and Hunderi[30] is valid only for small packing fractions and cannot be applied here.

IV. RESULTS AND DISCUSSIONS

Table I lists the packing fractions (volume fractions f_a) of each of the samples discussed in detail in this section. We list in addition the squares of the ordinary index of refraction n_0 of α-Al_2O_3 as given from the dispersion equation.[42] The birefringence (n_e-n_0) is of the order of 0.01 (Ref. 43) and was ignored since its effect was already small and would have been reduced to negligible proportions upon averaging. Moreover, the difference between the dielectric functions of the α and γ phase[44] is also negligible on our scale and was ignored. Also listed for comparison are the quasistatic EMA values of ϵ calculated at 5000 Å from Eq. (2) with the packing fractions appropriate to each sample. In this calculation we take $\epsilon_a=3.366$, f_a as given in Table I, $\epsilon_b=1$, $\epsilon_h=\epsilon$, and $q=\frac{1}{3}$. The EMA values change somewhat with wavelength owing to the dispersion in $\epsilon_a=n_0^2$.

A comparison of the results for the samples of particle sizes 0.05 and 0.3 μm is shown in Fig. 2. To eliminate as far as possible the effects of packing fraction and dispersion in the index of refraction, and thereby to make the comparison more meaningful, each datum of Table I was normalized before display in Fig. 2 by the appropriate EMA value of ϵ for that packing fraction and wavelength.

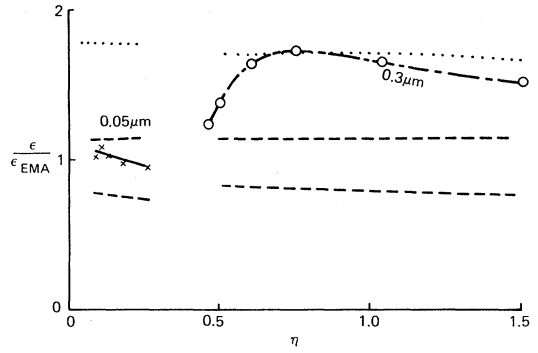

FIG. 2. Dielectric functions ϵ vs $\eta=d/\lambda$ of compressed Al_2O_3 pellets of particle sizes 0.05 and 0.3 μm, normalized to the quasistatic EMA values as described in the text. The quasistatic Hashin-Shtrikman and Wiener limits are shown as the dashed and dotted lines, respectively.

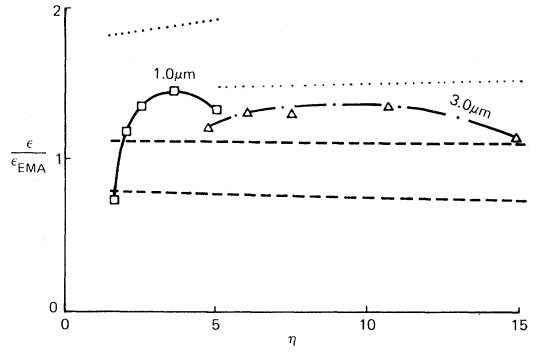

FIG. 3. Same as Fig. 2, but for the compressed Al_2O_3 pellets of particle sizes 1.0 and 3.0 μm.

Further rationale for this procedure is that the Hashin-Shtrikman limits, the absolute bounds to ϵ within the quasistatic theory for the packing fractions given, become essentially independent of both f_a and λ if this normalization is performed. These limits are shown in Fig. 2 as the dashed lines. The upper Wiener limits, corresponding to solid Al_2O_3, are shown as dotted lines for both samples. Lines are drawn through the experimental points only for clarity. A similar display for the samples of particle size 1.0 and 3.0 μm is shown in Fig. 3.

Several conclusions follow immediately from Figs. 2 and 3. First, the results for the 0.05-μm particle sample are in good agreement with quasistatic predictions. The values cluster about the normalized EMA value of 1.00, and to within the experimental uncertainty also fall between the normalized Bergman-Milton limits (the Maxwell-Garnet values) of 0.948 and 1.042. The results therefore favor the EMA value, as expected from an aggregate topology. The second qualitative conclusion is that for values of d/λ in excess of about 0.5, the measured values of ϵ are too large from the standpoint of the quasistatic theory. With the exception of the single 6328-Å point for the 1.0-μm particle samples (see below), *all* the data lie above the maximum value possible for the quasistatic theory. This is in qualitative agreement with the predictions of the laminar model which indicates that the waves tend to become evanescent in the less dense phase and that the energy tends to concentrate in the more dense material.

While the trends in Figs. 2 and 3 are clear, there exist some systematic differences that we thought might be attributable to the optical-system geometry. All data show an initial increase followed by a decrease for shorter wavelengths for measurements made with 13-mm beam diameters. The initial increase is most pronounced for the 0.3- and 1.0-μm particle sizes, i.e., those whose dimensions are also closest to the wavelength of light. Since the laser beam diameter without beam expander was 0.8 mm, an area of this diameter was delineated for additional Brewster-angle measurements. The lower coherence (incandescent lamp) system achieved the same delineation area with an aperture stop on the sensor side, thus assuring the Brewster-angle determination of the same areas. Comparisons with measurements using the standard tungsten-halogen source and corresponding beam-expanded laser (13 mm) source verified that the low initial values were not a result of the combination of the coherence of the laser source and the aperture

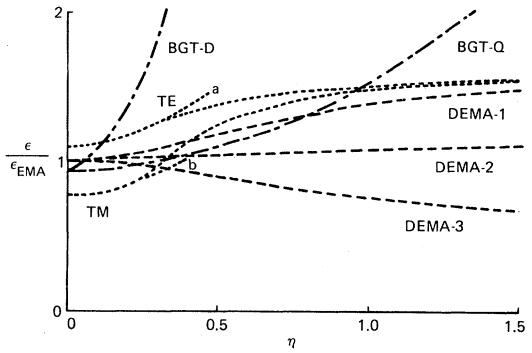

FIG. 4. Variations of ϵ with $\eta = d/\lambda$ calculated for parameters appropriate to the 0.3-μm particle sample at 4000 Å and normalized to the Bruggeman quasistatic values, as described in the text. The models are: BGT-*D*,BGT-*Q*: Bosi *et al.* dipole and quadrupole; TE,TM: laminar transverse electric and magnetic; DEMA-1, -2, and -3: dynamic EMA with spherical inclusions, spherical inclusions and voids, and spherical voids, respectively. Only the quadratic expansion is available for BGT-*D* and BGT-*Q*. Both quadratic and exact calculations are shown for the laminar model, while only exact calculations are shown for DEMA-1, -2, and -3.

stop on the sensor side of the system. A third set of measurements involving the smaller illumination areas at 6328 Å and no aperture stop on the sensor side of the system yielded no differences (± 0.02) for samples consisting of 0.05- and 3.0-μm particles. However, measurements on the 0.3- and 1.0-μm samples showed dependence on the illumination area. Repeatable values of ϵ as low as 1.83 (compared to 2.637, Table I) and as high as 1.75 (compared to 1.357, Table I) were observed on 0.3- and 1.0-μm samples, respectively, for the laser spot size of 0.8-mm diameter, although the 0.1- and 3.0-μm values did not change. If this effect is attributable to interference effects between the top two layers of the pressed sample, an analogy could be made to the Bragg law for interference in uniformly spaced lattices. Thus, as d (the particle size) increases, the diffraction angle decreases and the complementary Brewster angle increases as observed for the 1.0-μm particles; also, conversely for the 3.0-μm particles. Thus the dips at the onset of the 0.3- and 1.0-μm curves do not appear to be caused by an instrumental effect, but may be an interlayer interference effect.

We compare next the predictions of the theoretical models to our experimental results. Figure 4 shows the variations calculated from the laminar, DEMA, and perturbation models discussed in the preceding section. These models were evaluated us-

ing the parameters of the 0.3-μm particle-size sample at 4000 Å: $\epsilon_a = 3.411$, $f_a = 0.57$, and $\epsilon_b = 1$. The calculated values were normalized to the Bruggeman quasistatic value of ϵ to be able to compare Fig. 4 directly to Fig. 2. The exact solution for the laminar model[35] indicates that the quadratic terms should provide a reasonable representation for $d/\lambda < 0.5$ (Fig. 4: TE, *a* and TM, *b*). Beyond this range the higher-order terms cannot be neglected. Our purpose is simply to investigate trends in ϵ with increasing d/λ to see whether the models are reasonable. Note that the quasistatic limits differ among the models, as indicated previously.

Comparison with Fig. 2 shows that the variation predicted by the perturbation model of Bosi, Girouard, and Truong[36] (BGT) is too rapid to describe the data. The separate evaluation of magnetic dipole (BGT-*D*) and electric quadrupole (BGT-*Q*) terms shows that the magnetic dipole term is by far the larger and is primarily responsible for the disagreement between theory and experiment. The relative unimportance of quadrupole effects was also recognized in Ref. 36. Nevertheless, the inability of the formalism to represent the data shows that the approach is inadequate and that dynamic effects of this type cannot be treated as perturbations to quasistatic theories, but must be incorporated from the start.

The laminar model is compatible with the 0.3-μm particle results, but the initial rate of rise is too fast with respect to the 1.0- and 3.0-μm particle results. Moreover, the exact calculation shows that ϵ should essentially reach the Wiener limit for $d/\lambda = 1$, which is clearly incompatible with the 1.0-μm results of Fig. 3. This is not surprising, as the microstructure assumed in this model does not correspond to that of the actual samples.

We consider finally the full DEMA treatment given by Eq. (3.2) in Ref. 32. Although based on a spherical geometry, the allowance for regions with different diameters permits considerable flexibility in evaluating this expression. We show in Fig. 4 the results obtained in two limits: spherical polarizable regions of equal diameters (DEMA-1) and spherical *voids* of equal diameters (DEMA-3). Surprisingly, ϵ decreases with increasing d/λ in the latter case. This, however, is seen from Eq. (4) to be a natural consequence whenever $\epsilon > \epsilon_i$ for the dominant spherical inclusions. Assuming both inclusions and voids to be spherical with equal diameters (a topological impossibility, but shown as DEMA-2) produces a mean value giving a slow increase of ϵ with d/λ. In fact, the experimental topology should be appropriate to a variation somewhere between DEMA-1 and DEMA-2, recognizing that the actual particles are platelets, not spheres. This appears to be consistent with the results of both Figs. 2 and 3. However, our main point is to show that finite-wavelength theories encompass qualitatively different ranges of behavior depending on the microstructure, and therefore would be expected to have diagnostic value. Hereto, the quadratic approximation given by Eq. (4) is inaccurate, predicting too great a change.

It should be noted that the flexibility of finite-wavelength formalisms is inherently much greater than that of their quasistatic limits. Thus attempts to determine which of these formulations is "best" will be more difficult and less convincing than similar efforts applied to quasistatic theories. However, by deliberately choosing a system where the spectral dependence is secondary and the independent variable is d/λ, we have taken a novel approach and have succeeded in showing that a perturbative treatment is not adequate. Our results therefore provide insight towards more general representations of the dielectric response of composite media at finite frequencies.

V. SUMMARY AND CONCLUSIONS

Our results can be summarized briefly as follows. For particle diameter to wavelength ratios $\eta = d/\lambda \lesssim 0.25$, the mean-field theories[2–10] give an adequate description of the data. Of the possible mean-field theories, the Bruggeman effective-medium approximation[4] (EMA) for the three-dimension isotropic case most accurately matches the data, as expected for aggregate configurations. For larger values of d/λ, ϵ increases in value over the mean-field value in qualitative agreement with the focusing or waveguiding effect that is active in laminar configurations.[35] The rate of increase is consistent with the predictions of the dynamic effective-medium approximation (DEMA) of Stroud and Pan,[32] which is itself a special case of a more general theoretical treatment by Lamb, Wood, and Ashcroft.[34] We find that the changes in ϵ with increasing d/λ are sensitive to microstructure. Specifically, we find that in theory ϵ can either increase or decrease with increasing d/λ according to whether the voids, the polarizable constituents, or both are considered spherical. In fact, our Al_2O_3 composites composed of platelets behave by this criterion as if both particles and voids have a basically

spherical microstructure.

Our results show that the perturbation model of Bosi, Girouard, and Truong,[36] wherein finite-wavelength effects are treated as time-dependent dipolar and quadrupolar corrections to a quasistatic solution, is not compatible with our experimental results even though here the microstructure assumed theoretically *is* consistent with experiment. The rate of increase of ϵ with d/λ predicted by this model is considerably larger than that calculated in the laminar approach and also far larger than experiment. The prediction of more rapid changes than those obtained for a special microstructure for which screening was maximized indicates quite clearly that finite-wavelength effects generally cannot be incorporated as additions to electrostatic theories but must be included in the initial formulation of the effective-medium problem.

[1]See, e.g., for a survey, R. Landauer, in *Electrical Transport and Optical Properties of Inhomogeneous Media—1977 (Ohio State University, Ohio)*, Proceedings of the First Conference on the Electrical Transport and Optical Properties of Inhomogeneous Media, edited by J. C. Garlard and D. B. Tanner (AIP, New York, 1978), p. 2.

[2]L. Lorenz, Ann. Phys. Chem. (Leipzig) 11, 70 (1880); H. A. Lorentz, *Theory of Electrons*, 2nd ed. (Teubner, Leipzig, 1916).

[3]J. C. Maxwell-Garnett, Philos. Trans. R. Soc. London 203, 385 (1904); Philos. Trans. R. Soc. London Ser. A 205, 237 (1906).

[4]D. A. G. Bruggeman, Ann. Phys. (Leipzig) 24, 636 (1935).

[5]G. V. Rozenberg, Usp. Fiz. Nauk. 69, 59 (1959).

[6]D. Bedeaux and J. Vlieger, Physica (Utrecht) 73, 287 (1974).

[7]M. Omini, Physica (Utrecht) 83A, 431 (1976); 84, 129 (1976); 84, 142 (1976).

[8]R. Brako, J. Phys. C 11, 3345 (1978).

[9]G. B. Smith, Appl. Phys. Lett. 35, 668 (1979).

[10]F. A. Bondar, Thin Solid Films 81, 121 (1981).

[11]O. Wiener, Abh. Math.-Phys. Kl Saechs. Ges. 32, 509 (1912).

[12]Z. Hashin and S. Shtrikman, J. Appl. Phys. 33, 3125 (1962).

[13]D. J. Bergman, Phys. Rev. Lett. 44, 1285 (1980).

[14]G. W. Milton, Appl. Phys. Lett. 37, 300 (1980).

[15]D. E. Aspnes, Thin Solid Films 89, 249 (1982).

[16]C. G. Granqvist and O. Hunderi, Phys. Rev. B 16, 3513 (1977).

[17]C. Grosse and J. L. Greffe, J. Chim. Phys. 76, 305 (1979).

[18]D. E. Aspnes, J. B. Theeten, and F. Hottier, Phys. Rev. B 20, 3292 (1979).

[19]G. A. Niklasson, C. G. Granqvist, and O. Hunderi, Appl. Opt. 20, 26 (1981).

[20]U. Kreibig, J. Phys. F 4, 999 (1974).

[21]J. I. Gittleman and B. Abeles, Phys. Rev. B 15, 3273 (1977).

[22]C. G. Granqvist and O. Hunderi, Phys. Rev. B 18, 2897 (1978).

[23]S. Norrman, T. Andersson, C. G. Granqvist, and O. Hunderi, Phys. Rev. B 18, 674 (1978).

[24]P. O'Neill and A. Ignatiev, Phys. Rev. B 16, 6540 (1978).

[25]D. E. Aspnes, E. Kinsbron, and D. D. Bacon, Phys. Rev. B 21, 3290 (1980).

[26]S. Santucci, P. Picozzi, L. Paoletti, and F. Tangucci, Thin Solid Films 79, 133 (1981).

[27]B. G. Bagley, D. E. Aspnes, A. C. Adams, and F. B. Alexander, Appl. Phys. Lett. 38, 56 (1981).

[28]C. G. Granqvist, Appl. Opt. 20, 2606 (1981).

[29]U. J. Gibson, H. G. Craighead, and R. A. Buhrman, Phys. Rev. B 25, 1449 (1982).

[30]C. G. Granqvist and O. Hunderi, Phys. Rev. B 16, 1353 (1977).

[31]R. Ruppin, Phys. Status Solidi B 87, 619 (1978).

[32]D. Stroud and F. P. Pan, Phys. Rev. B 17, 1602 (1978).

[33]C. M. Horwitz, J. Opt. Soc. Am. 68, 1032 (1978).

[34]W. Lamb, D. M. Wood, and N. W. Ashcroft, Phys. Rev. B 21, 2248 (1980).

[35]D. E. Aspnes, Phys. Rev. B 25, 1358 (1982).

[36]G. Bosi, F. E. Girouard, and V.-V. Truong, J. Appl. Phys. 53, 648 (1982).

[37]A. Ignatiev, P. O'Neill, C. Doland, and G. Zajac, Appl. Phys. Lett. 34, 42 (1979).

[38]W. G. Egan and T. Hilgeman, Appl. Opt. 19, 3724 (1980).

[39]G. B. Smith, Appl. Phys. Lett. 35, 668 (1979).

[40]W. G. Egan and T. W. Hilgeman, *Optical Properties of Inhomogeneous Materials* (Academic, New York, 1979).

[41]G. Mie, Ann. Phys. 25, 377 (1908).

[42]I. H. Malitson, J. Opt. Soc. Am. 52, 1377 (1962).

[43]V. Chandrasekharan and H. Damany, Appl. Opt. 7, 939 (1968).

[44]*Eigenschaften der Materie in Ihren Aggregatzuständen, Optische Konstanten,* Vol. 8 of *Landolt-Börnstein Zahlenwerte und Funktionen, II,* edited by K.-H. Hellwege and A. M. Hellwege (Springer, Berlin, 1962).

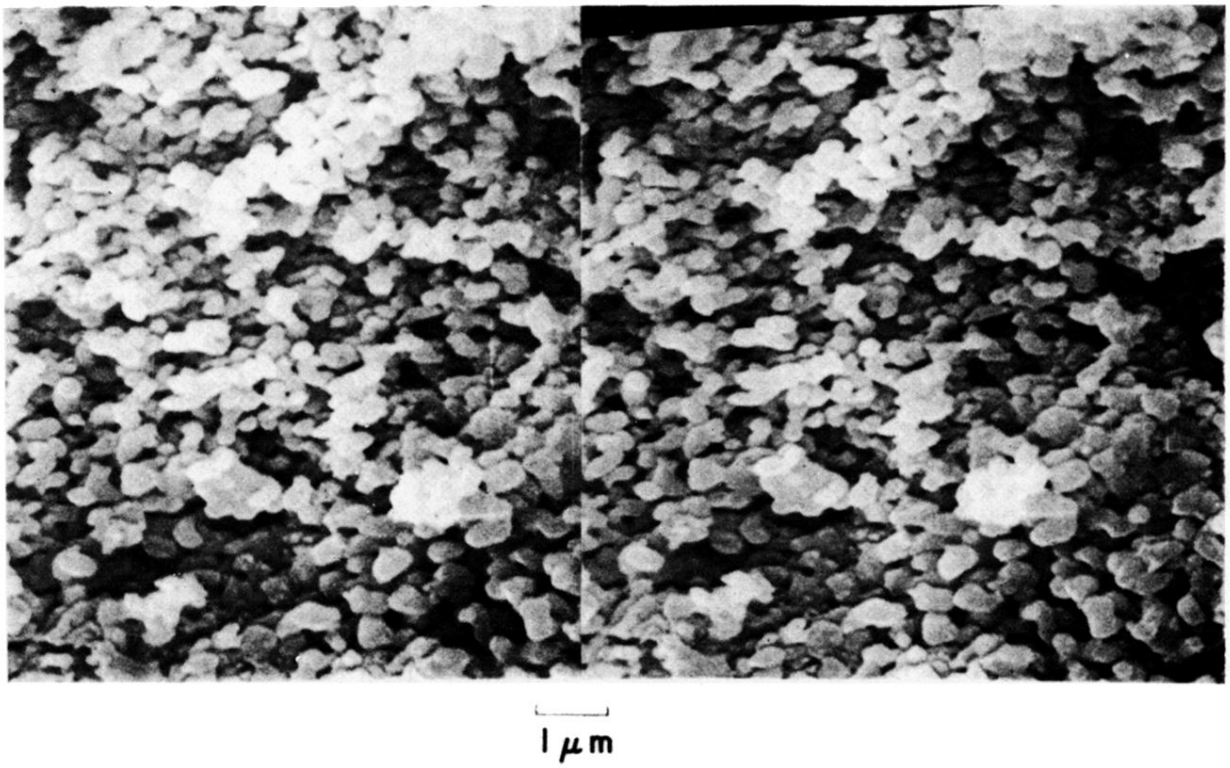

FIG. 1. Stereographic SEM micrographs of the front surface of a pressed-powder composite prepared from 0.3-μm alumina abrasive. The surface can be seen in three dimensions by using a stereo viewer.